CALIBRATION OF ELASTIC-PLASTIC MATERIAL MODEL FOR TIRE SHREDS

Boris Jeremić* Member, ASCE,
James Putnam† Member, ASCE,
Kallol Sett‡ Student Member, ASCE,
Dana Humphrey§ Member, ASCE,
Stacey Patenaude¶

October 22, 2010

Abstract

In this paper we present the development of an elastic-plastic material model for tire shreds material. In particular, our aim is to use large scale triaxial tests to calibrate the elastic and elastic-plastic model for this anisotropic material. The main effort is focused on the dynamic behavior of tire shred material and in particular the energy dissipation characteristics during dynamic (seismic) loading. This paper presents results of a material model calibration using wave propagation tests on a triaxially loaded tire shred specimen.

The immediate goal of the presented work is the creation of a verified and validated elastic-plastic material model that will then be used in numerical assessment of seismic behavior of bridge abutments. The validation procedure will ultimately include simulations of two bridge abutments made of tire shreds performed using a large centrifuge facility at UC Davis.

1 Introduction

Civil engineering application is a growing market for scrap tires. Scrap tires have been successfully used as light-weight fill [HM92]; [THS98]; [HN97], insulation beneath roads [HE95], light-weight backfill for retaining walls [THS98], overlay of underground ramps or storage space [HD99], and as stream crossing [Geb97], primarily because of low unit weight, high permeability and good insulating properties.

*Department of Civil and Environmental Engineering, University of California, Davis, CA 95616. jeremic@ucdavis.edu
†Department of Civil and Environmental Engineering, University of California, Davis, CA 95616.
‡Department of Civil and Environmental Engineering, University of California, Davis, CA 95616.
§Department of Civil and Environmental Engineering, University of Maine, Orino, ME 04469.
¶California Integrated Waste Management Board, Sacramento, CA 95812.

The placement and compaction of tire shreds leads to a layered, anisotropic material behavior. Isotropic deformability parameters and time-dependent creep behavior of tire-shreds were reported in the past by several researchers [HM92]; [HE95]; [THS98]; [HD98]; however, only a few studies have been carried out to evaluate anisotropic properties of a tire shred model. Heimdahl and Drescher (1999) first attempted to develop an elastic anisotropic model for tire shred behavior using a biaxial testing apparatus. They reported over a dozen plane stress tests at two loading conditions and averaged the elastic constants thus determined. A large variation of in-plane Poisson's ratio was reported with the possibility of negative values discussed. The authors acknowledged that the test apparatus employed was not the best for determining Poisson's ratio.

This paper deals with the development of an elastic-plastic material model for the tire shred material. In particular, our aim was to use a large scale triaxial testing apparatus, developed at University of California, Davis to calibrate the elastic and elastic-plastic material model for anisotropic material. Our immediate goal was to create, verify and validate an elastic-plastic material model that can then be used in numerical assessment of seismic behavior of bridge abutments. The validation procedure will ultimately include computational and experimental simulations of two bridge abutments made of tire shreds, performed using a large centrifuge facility at UC Davis.

2 Elastic Cross-Anisotropic Constitutive Law

The linear, small-strain, elastic behavior of cross-anisotropic material is governed by the following generalized Hooke's law [HD99]:

$$\epsilon_{11} = \frac{1}{E}\sigma_{11} - \frac{E-2G}{2GE}\sigma_{22} - \frac{E'-2G'}{2G'E'}\sigma_{33} \tag{1}$$

$$\epsilon_{22} = -\frac{E-2G}{2GE}\sigma_{11} + \frac{1}{E}\sigma_{22} - \frac{E'-2G'}{2G'E'}\sigma_{33} \tag{2}$$

$$\epsilon_{33} = -\frac{E-2G''}{2G''E}\sigma_{11} - \frac{E-2G''}{2G''E}\sigma_{22} + \frac{1}{E'}\sigma_{33} \tag{3}$$

$$\epsilon_{23} = \frac{1}{2G''}\sigma_{23} \quad ; \quad \epsilon_{13} = \frac{1}{2G''}\sigma_{13} \quad ; \quad \epsilon_{12} = \frac{1}{2G}\sigma_{12} \tag{4}$$

where, in equation (1) $E = E_{11}$ = in-plane Young's modulus; $E' = E_{33}$ = out-of-plane Young's modulus; $G = G_{12}$ = in-plane shear modulus; $G' = G_{31}$ = out-of-plane shear modulus; $G'' = G_{13}$ = out-of-plane shear modulus. Note that "in-plane" refers to the 1-2 isotropy plane (horizontal) and "out-of-plane" refers to the 3-direction (assumed vertical).

The above elastic material constants, E, E', G, G', and G'' can be determined from three-dimensional P-wave and shear wave tests. The equation relating in-plane Young's modulus (E) and in-plane P-wave velocity (V_{c_i}; $i = 1, 2$) is,

$$E = \rho V_{c_i}^2 \tag{5}$$

Similarly, the equation relating out-of-plane Young's modulus (E') and out-of-plane P-wave velocity (V_{c_3}) is,

$$E' = \rho V_{c_3}^2 \tag{6}$$

The equation relating in-plane shear modulus (G) and in-plane shear wave velocity with horizontal polarization ($V_{s_i}^H$; $i = 1,2$) is,

$$G = \rho (V_{s_i}^H)^2 \tag{7}$$

where wave propagation is in the i-direction (i=1,2) with horizontal polarization. The equation relating out-of-plane shear modulus (G') and out-of-plane shear wave velocity (V_{s_3})is,

$$G' = \rho (V_{s_3})^2 \tag{8}$$

where wave propagation is in the 3-direction with horizontal polarization. Finally, the equation relating out-of-plane shear modulus (G'') and in-plane shear wave velocity with vertical polarization ($V_{s_i}^V$; $i = 1,2$) is,

$$G'' = \rho (V_{s_i}^V)^2 \tag{9}$$

where wave propagation is in the i-direction ($i = 1,2$) with vertical polarization.

3 Elastic-Plastic Constitutive Law

The most general form of elastic-perfectly plastic incremental stress-strain relationship can be expressed as [CH88],

$$d\sigma_{ij} = C_{ijkl}^e p d\epsilon_{kl} \qquad \text{where} \qquad C_{ijkl}^e p = C_{ijkl} - \frac{C_{ijmn}\dfrac{\partial f}{\partial \sigma_{mn}}\dfrac{\partial f}{\partial \sigma_{pq}}C_{pqkl}}{\dfrac{\partial f}{\partial \sigma_{rs}}C_{rstu}\dfrac{\partial f}{\partial \sigma_{tu}}} \tag{10}$$

The coefficient tensor $C_{ijkl}^e p$ is the elastic-plastic tensor of tangent moduli for an elastic-perfectly plastic material. The tensor of elastic moduli, C_{ijkl}, can be expressed in terms of E and ν as [CH88],

$$C_{ijkl} = \frac{E}{2(1+\nu)}\left[\frac{2\nu}{(1-\nu)}\delta_{ij}\delta_{kl} + \delta_{ik}\delta_{jl} + \delta_{il}\delta_{jk}\right] \tag{11}$$

By using Hooke's law and additive decomposition of strain tensors in the elastic and plastic parts [JS97] we obtain

$$d\sigma_{ij} = C_{ijkl} d\epsilon_{kl} - d\lambda C_{ijkl}\frac{\partial f}{\partial \sigma_{kl}} \tag{12}$$

By substituting Eq. (11) into Eq. (12), and with $\nu = (1/2)(3K - 2G)/(3K + G)$ it follows

$$d\sigma_{ij} = 2G d\epsilon_{ij} + K d\epsilon_{kk}\delta_{ij} - d\lambda\left[\left(K - \frac{2}{3}G\right)\frac{\partial f}{\partial \sigma_{mn}}\delta_{mn}\delta_{ij} + 2G\frac{\partial f}{\partial \sigma_{ij}}\right] \tag{13}$$

Assuming a Drucker-Prager material model, the yield function, f, is given by, $f(\sigma_{ij}) = F(I_1, \sqrt{J_2}) - K = 0$ and hence it follows that

$$\frac{\partial f}{\partial \sigma_{ij}} = \frac{\partial f}{\partial I_1}\delta_{ij} + \frac{1}{2\sqrt{J_2}}\frac{\partial f}{\partial \sqrt{J_2}}S_{ij} \tag{14}$$

Substituting Eq. (14) into Eq. (13) we have,

$$d\sigma_{ij} = 2Gd\epsilon_{ij} + Kd\epsilon_{kk}\delta_{ij} - d\lambda\left(3K\frac{\partial f}{\partial I_1}\delta_{ij} + \frac{G}{\sqrt{J_2}}\frac{\partial f}{\partial\sqrt{J_2}}S_{ij}\right) \tag{15}$$

where $d\lambda$ has the form,

$$d\lambda = \frac{3Kd\epsilon_{kk}\left(\frac{\partial f}{\partial I_1}\right) + \left(\frac{G}{\sqrt{J_2}}\right)\left(\frac{\partial f}{\partial\sqrt{J_2}}\right)S_{mn}d\epsilon_{mn}}{9K\left(\frac{\partial f}{\partial I_1}\right)^2 + G\left(\frac{\partial f}{\partial\sqrt{J_2}}\right)^2} \tag{16}$$

Now, the Drucker-Prager yield condition,f, is given by

$$f = \sqrt{J_2} + \alpha I_1 - k = 0 \tag{17}$$

Combining Eqs. (15), (16) & (17), we have the most general form of Drucker-Prager elastic-perfectly plastic constitutive relationship as,

$$\begin{aligned} d\sigma_{ij} &= \Bigg[2G\delta_{im}\delta_{jn} + \left(K - \frac{2}{3}G\right)\delta_{ij}\delta_{mn} - \\ &\quad \frac{\left(\frac{G}{\sqrt{J_2}}\right)S_{ij} + 3K\alpha\delta_{ij}}{G + 9K\alpha^2}\left(\frac{G}{\sqrt{J_2}}S_{mn} + 3K\alpha\delta_{mn}\right)\Bigg]d\epsilon_{mn} \end{aligned} \tag{18}$$

This relationship will be used in assessing one dimensional wave propagation characteristics of tire shred material described below.

4 Material and Methods

The concept of triaxial testing of tire shreds has been considered by some and easily dismissed because of the material and equipment logistics required. At UC Davis, a large sample triaxial compression specimen was successfully developed and used for testing P-wave and shear wave (S-wave) propagation characteristics.

4.1 Material

The size of tire shreds, provided by the California Integrated Waste Management Board (CIWMB), ranged from about 30 cm long by 5 cm wide by 0.8 cm thick (long and thin) to about 10 cm long by 5 cm wide by 5 cm thick (massive rubber) to about 3 cm long by 2 cm wide by 0.8 cm thick (chips). A trace of tire crumbs (2 to 5 mm size) was also noted. These dimensions are typical of routine tire shredding operations. The specific gravity of the tire shreds was determined to be about 1.20. The variation in porosity from loosest to densest was estimated as 0.68 to 0.49.

4.2 Methods

The compaction mold for a large triaxial test specimen of tire shreds was fabricated from a 1.2 m inside-diameter polypropylene culvert (provided by CIWMB); 1.25 mm latex sheeting was used to fabricate the triaxial test membrane. The end platens were 25 mm (top platen) and 12.5 mm (bottom platen) thick steel plates. The load frame was an existing structural steel frame used for consolidating large soil samples at the National Geotechnical Centrifuge at UC Davis. Vertical load was provided by dual-acting, 76 mm-diameter, hydraulic rams with a 76 cm-stroke and a maximum operating pressure of about 20 MPa. Vacuum loading for confining pressure was provided using a high-volume Thomas Industries H50A-60 vacuum generator working off air pressure. Instrumentation for measurement of P- and S-waves consisted of 42 piezoelectric, ICP accelerometers by PCB Piezotronics.

After the latex membrane was secured to the bottom platen, the mold was secured in place and the combined apparatus was placed on a specially fabricated lifting frame to provide a solid stable base for the bottom platen to rest on during sample preparation. Two horizontal and two vertical rows of accelerometer arrays were established as shown schematically in Fig. 1.

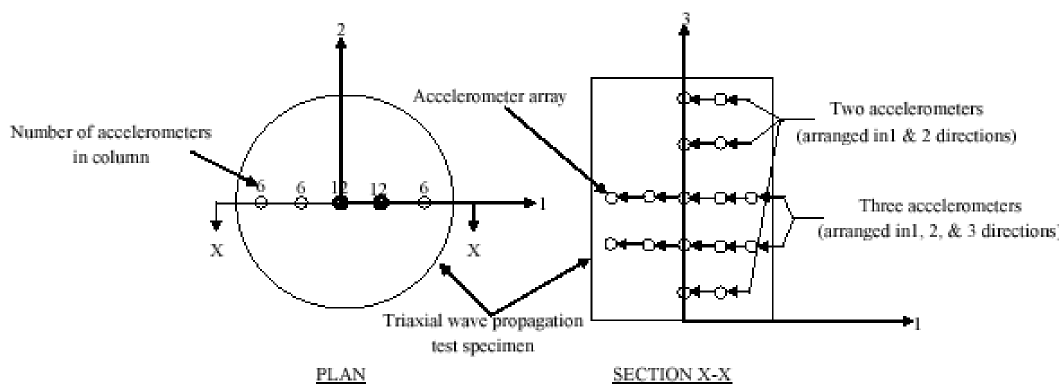

Figure 1: Schematic of Accelerometer Arrays

The tire shreds were placed in approximately 150 mm lifts, about 100 kg per lift, and compacted with a walk-behind vibrating plate compactor (Wacker model) with a 172 kg static weight. As each lift was brought to the level of accelerometer placement, precise accelerometer locations were determined using a pre-marked rod and plumb bob. The completed triaxial test set up, placed in the load frame, is shown in Fig. 2.

As discussed earlier, the directional Young's moduli and shear moduli were obtained from three-dimensional P- and S- wave velocities. The P- and S- waves were generated by striking appropriately positioned metal or PVC striker blocks (either welded to the top and bottom

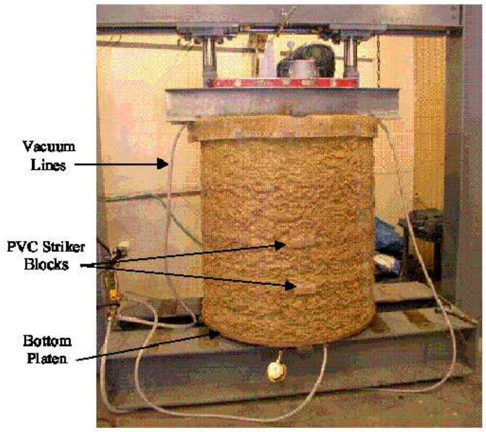

Figure 2: Triaxial Test Set Up

platens or inserted during specimen preparation) with a 0.5 kg, double-headed 'dead blow' hammer. The P- and S- wave velocities were measured through the accelerometer arrays shown in Fig. 1 and recorded via a data acquisition system with a scan rate of 10,000 readings per second from each accelerometer. To model in situ conditions, the embankment profile shown in Table 1 was assumed. The tire shred specimen was tested under four triaxial load conditions representing the top and bottom of each tire shred layer as tabulated in Table 1. Table 2 presents the loading conditions modeled during our testing.

Table 1: Assumed Embankment Profile

Thickness [m]	Material	Density [Mg/m^3]
1.2	Paving and compacted soil	2.0
3	Tire shreds	0.8
1	Compacted soil	2.0
3	Tire shreds	0.8

Table 2: Selected Loading Conditions for Tests

load number	σ_v [kPa]	σ_h [kPa]	K_0
1	23.9	11.3	0.47
2	47.9	13.4	0.28
3	65.8	18.4	0.28
4	89.9	25.1	0.28

5 Test Results and Discussions

A total of 83 tests were performed from different wave source locations. Because the data acquisition system was limited to 16 channels, several unload-reload cycles were required for each load condition. Unfortunately this load cycling resulted in excessive deformation of the test specimen. Although some accelerometer response was lost due to excessive deformation, useful data were obtained for the first three load cases. The in-plane Young's modulus ($E_{11} = E_{22} = E$) and the out-of-plane Young's modulus ($E_{33} = E'$) were calculated from Eq. (5) and Eq. (6). The in-plane Poisson's ratio ($\nu_{12} = \nu_{21}$) was calculated from the in-plane shear modulus Eq.(7) and in-plane Young's modulus as,

$$\nu_{12} = \frac{E_{11}}{2G_{12}} - 1 \tag{19}$$

The out-of-plane Poisson's ratios (ν_{31} and ν_{13}) were calculated from the in-plane Young's modulus (E_{11}), out-of-plane Young's modulus (E_{33}), and out-of-plane shear moduli, $G'' = G_{13}$ (Eq. 9) and $G' = G_{31}$ (Eq. 8) as

$$\nu_{31} = \frac{E_{33}}{2G_{31}} - 1 \quad ; \quad \nu_{13} = \frac{E_{11}}{2G_{13}} - 1 \tag{20}$$

To describe the behavior of a cross-anisotropic material, five independent elastic constants are required. All other constants can be defined from these five independent constants. In this study the redundant constants are calculated either for use in the elastic-plastic material model Eq. (22) or to cross-check with published data [HD99]. The test results are tabulated in Table 3.

Table 3: Elastic Constants

load	σ_v	σ_h	G_{31}	G_{13}	E_{33}	$E_{11,22}$	E_{11}/E_{33}	ν_{12}	ν_{13}	ν_{31}
1	23.9	11.3	1500	1820	3330	5000	1.5	0.11	0.37	0.11
2	47.9	13.4	2550	5320	3825	9000	2.35	0.22	-0.15	-0.25
3	65.8	18.4	4890	19440	3835	13000	3.39	0.33	-0.67	-0.6

The current testing program shows that the computed G_{31} is equal to the computed G_{32}, as would be expected for a cross-anisotropic material. The testing also shows that E_{11} was greater than E_{33}, and that the ratio appears to increase with increased loading. Thus the data appears to confirm the cross-anisotropic assumption proposed for the layered tire shred model. Indeed, the results indicate a stress-induced anisotropy, i.e., the anisotropy increases with increased stress. It is also noted that the measured negative Poisson's ratio, while physically possible, may be open for discussion. This will be investigated in the next set of tests that are forthcoming in early 2004. It is suspected that the increase of confinement from the stretched latex membrane may have added some error to calculating Poisson's ratios.

6 Elastic-Plastic Model and Correlation with $\mathbf{G/G_{max}}$

The general form of three-dimensional Drucker-Prager elastic-plastic constitutive relationship Eq. (18) can be simplified to any direction of interest. Thus, knowing the current state of the stress tensor and strain-increment in that particular direction, the stress increment in that direction can be solved for incrementally to get the elastic-plastic stress-strain relationship.

For the case of shear wave propagation in the 3-direction with horizontal polarization Eq. (18) can be simplified to the following form by substituting $i = 3$; $j = 1$; $m = 3$ and $n = 1$, which after some tensor algebra becomes:

$$d\sigma_{31} = \left[2G_{31} - \frac{\frac{G_{31}^2}{J_2}}{G_{31} + 9K\alpha^2} S_{31} S_{31} \right] d\epsilon_{31} \tag{21}$$

The bulk modulus, K, is calculated from E_{11}, E_{33}, ν_{12}, ν_{31}, using the relationship,

$$K = \frac{1}{3\left(\dfrac{1}{E_{11}} - \dfrac{\nu_{12}}{E_{11}} - \dfrac{\nu_{31}}{E_{33}} \right)} \tag{22}$$

The Drucker-Prager material constant, α, is related to the friction angle, ϕ, as,

$$\alpha = \frac{2\sin\phi}{\sqrt{3}(3 - \sin\phi)} \tag{23}$$

Knowing E_{11}, E_{33},ν_{12}, ν_{31} (Table 3) and using $\phi = 20^0$ [THS98] Eq. (21) was solved incrementally and the predicted elastic-plastic stress (τ_{31})-strain (γ_{31}) relationship is shown in Fig. 3(a).

Eq. (21) also represents the variation of G/G_{max} which is usually found in traditional analysis of dynamics of soils. The term inside the bracket in Eq. (21) is the elastic-plastic shear modulus, which is dependent on the stress deviator and reduces with increase in stress/strain. Fig. 3(b) shows the predicted reduction of shear modulus in terms of dimensionless parameters G_{31}/G_{31max} versus γ_{31}.

7 Conclusions

Based on this experimental and theoretical study, the following conclusions can be advanced:

1. Three-dimensional triaxial P- and S-wave velocity testing can be used to determine the five elastic constants necessary for modeling the behavior of anisotropic tire shred material.

2. The test results demonstrated the cross-anisotropic nature of the tire shred material. It was also observed that anisotropy increased with stress (stress-induced anisotropy).

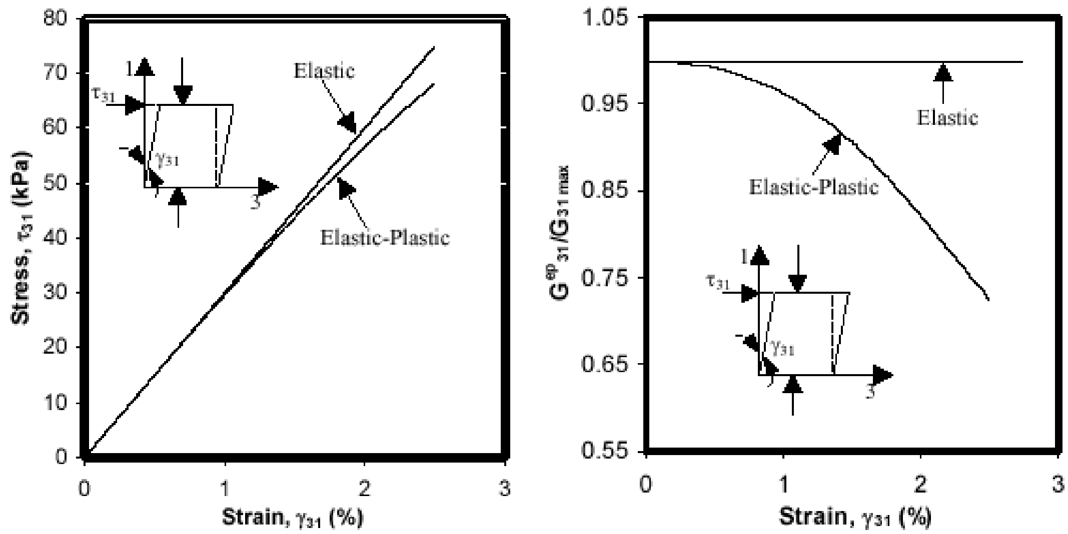

Figure 3: (a) Predicted Elastic and Elastic-Plastic Stress-Strain Relationship; (b) Predicted Variation of Shear Modulus with Strain

3. The data obtained from three-dimensional triaxial P- and S- wave propagation tests can be used to calculate an elastic-perfectly plastic material model for the tire shreds material. The model also represented the variation of G/G_{max}, that is usually found in traditional analysis of dynamics of frictional media.

4. Further testing is necessary to mitigate the excessive deformation caused by unload-reload cycles in the current program. Additional testing would also target redundant measurements of six elastic constants so as to evaluate the negative Poisson's ratio determinations from the current program.

8 Acknowledgment

This work was supported by the California Integrated Waste Management Board Special Waste Division (part of California Environmental Protection Agency) award # IWM-C0141/02-00296V.

References

[CH88] W.F. Chen and D.J. Han. *Plasticity for Structural engineers.* Springer-Verlag, 1988.

[Geb97] Megan Alissa Gebhardt. Shear strength of shredded tires as applied to the design and construction of a shredded tire stream crossing. Master's thesis, Iowa State University, Ames, Iowa, 1997.

[HD98] T. C. Heimdahl and A. Drescher. Deformability parameters of lightweight fills. In *9th Conference of Cold Region Engineering*, pages 524–535, Duluth, Minn., 1998. ASCE.

[HD99] Thor C. Heimdhal and Andrew Drescher. Elastic anisotropy of tire shreds. *Journal of Geotechnical and Geoenvironmental Engineering*, pages 383–389, May 1999.

[HE95] D.N. Humphrey and R.A. Eaton. Field performance of tire chips as subgrade insulation for rural roads. In *Proc., 14th International conference on Low-Volume Roads*, volume 2, pages 77–86. TRB, National Research Council, Washington, D.C., 1995.

[HM92] D. N. Humphrey and W. P. Manion. Properties of tire chips for lightweight fill. In R. H. Borden et al, editor, *Proc., Conf. on Gouting, soil improvement and geosynthetics*, volume 2, pages 1344–1355, ASCE, New York, 1992.

[HN97] D.N. Humphrey and Jr. W.L. Nickels. Effect of tire chips as lightweight fill on pavement performance. In *Proc., 14th International Conference on Soil Mechanics and Foundation Engineering*, volume 3, pages 1617–1620, 1997.

[JS97] Boris Jeremić and Stein Sture. Implicit integrations in elasto–plastic geotechnics. *International Journal of Mechanics of Cohesive–Frictional Materials*, 2:165–183, 1997.

[THS98] J.J. Tweedie, D.N. Humphrey, and T.C. Sanford. Tire shreds as lightweight retaining wall backfill: Active condition. *Journal of Geotechnical and Geoenvironmental Engineering*, pages 1061–1070, November 1998.